QUANTITATIVE 3D TEXTURAL AND PETROFABRIC ANALYSIS OF THE NORTHWEST AFRICA 10645 NAKHLITE USING X-RAY COMPUTED TOMOGRAPHY. S. Ramsey[1], A. Udry[1], S. Eckley[2], R. Ketcham[3]. [1]Department of Geoscience, University of Nevada, Las Vegas, Las Vegas NV, USA; ramses3@unlv.nevada.edu. [2]Jacobs, NASA JSC, Houston, TX, USA. [3]Jackson School of Geosciences, University of Texas, Austin, TX, USA.

Introduction: Martian meteorites are currently the only samples available from Mars to study and are critical for elucidating variability in martian igneous processes over time [e.g., 1]. Quantifying igneous textures and fabrics can help us understand how rocks are formed and emplaced [e.g., 2]. These features are innately three dimensional (3D) and are often strongly heterogeneous in cumulate rocks, like the nakhlites and poikilitic shergottites [2–3], where there can be substantial textural variations between and within individual samples. However, most quantitative textural and fabric analyses on these samples have been limited to two dimensions through measurements made on polished petrographic thin sections. Thus, 3D petrographic measurements are imperative for both representative sample characterization and accurately interpreting magmatic processes. The emplacement of martian meteorites at or near the surface of Mars (i.e., extrusive or intrusive, respectively) remains enigmatic due to the innate lack of geologic context [e.g., 1], but conducting 3D quantitative textural and fabric analyses can help elucidate emplacement mechanisms and settings on Mars.

X-ray computed tomography (CT) is a non-destructive method to characterize objects in 3D and has seen an increase in popularity in geoscience and planetary science [e.g., 4–5], as it is ideal for studying rare samples like martian meteorites. We have acquired X-ray CT scans for seven nakhlites (Northwest Africa — NWA — 11013, NWA 10645, NWA 13669, Miller Range — MIL — 03346, MIL 090030, MIL 090032, and MIL 090136) and five poikilitic shergottites (NWA 7937, NWA 7755, NWA 11043, NWA 12241, and NWA 14673). Here, we focus on the nakhlite, NWA 10645, as we have completed both preliminary quantitative textural and petrofabric analyses to constrain the emplacement of this sample and make comparisons with existing 2D data.

Methods: X-ray CT scanning on an epoxy mount of NWA 10645 was conducted at the High-Resolution X-ray CT Facility at the University of Texas at Austin using a Zeiss Xradia 620 Versa scanner with a LE4 filter. Scan conditions included an X-ray source energy of 80 kV and X-ray power of 10 W. A total of 4501 projections were collected over a 360° rotation, and the reconstructed voxel (i.e., 3D pixel) size was 7.05 μm.

Modal abundances: The "Segmentation Wizard" tool in *Dragonfly*™ (Object Research Systems) was used to train a classifier on 12 manually segmented slices and 10 sub-slices of NWA 10645 to enable automatic segmentation of the entire dataset. The greyscale values of plagioclase and glass display substantial overlap, thus these phases have been combined as 'mesostasis.' Voxels were categorized as either air, mesostasis, pyroxene, olivine (+ phosphates), or highly attenuating (high-μ) phases (i.e., oxides and sulfides). Whole-rock and 2D slice-by-slice modal abundances were then determined using the segmented data in *ImageJ*. Whole-rock and slice-by-slice modal abundances were normalized to the total number of non-air voxels in the X-ray CT dataset. Due to sample shape and orientation, the first and last 150 slices were excluded from our 2D slice-by-slice analysis of NWA 10645 to avoid areas where only a few voxels were present.

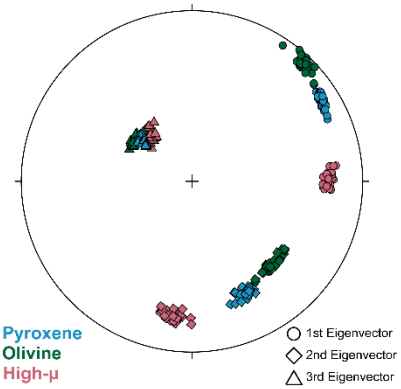

Figure 1. Stereonet showing the eigenvector orientations for each phase in NWA 10645 measured using *Quant3D*. High-μ phases include oxides and sulfides.

CT fabric analysis: Petrofabrics were quantified using our segmented CT scan and *Quant3D* [6], which measures the fabric of a segmented phase without separating individual crystals. As the test point placement in *Quant3D* is random, we performed 30 replicate analyses for each phase. Fabrics were visualized by plotting the eigenvectors of the replicate analyses on a stereonet (Fig. 1). Using the eigenvalues from *Quant3D*, we calculated the shape parameters, T and P' [7], for each phase. Phase alignment was determined using the eigenvectors.

3D crystal size distribution (CSD): To conduct a 3D pyroxene CSD, we oriented three orthogonal views of the X-ray CT scan in *Dragonfly*™ to find the long, intermediate, and short axes of each pyroxene crystal. Then, the shape of all pyroxene crystals (n=365) from a representative ~125 mm^3 rectangular prism sub-volume of NWA 10645 was approximated by manually drawing a rod through the center of each crystal using the multi-

slice round (i.e., spherical) brush tool, a method used successfully by [8]. Crystals that intersected the sub-volume boundary (n=117) or with center points outside the sub-volume boundary (n=72) were not included in our 3D CSDs (Fig. 2). Pyroxene rods using each technique (n=248 and 293) were then exported and separated in *Blob3D* [9] to extract dimensional (i.e., long axis length) data. Note that we first attempted to use *Blob3D* for the entirety of our 3D CSD, but separating touching and intergrown pyroxene crystals in the segmented NWA 10645 CT dataset was not feasible.

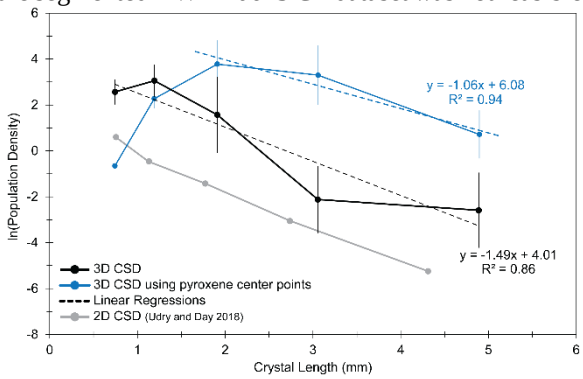

Figure 2. Crystal size distribution plot for NWA 10645 pyroxene with both 3D (this study) and 2D [2] results shown. Dashed lines are linear regressions through the 3D data to determine CSD slope and *y*-intercept.

Results: *Modal abundances*: Whole-rock 3D modal abundances for NWA 10645 are as follows: 59% pyroxene, 15% olivine and phosphates, 25% mesostasis, and 1% high-μ phases. The average 2D modal abundances are 65% pyroxene, 9% olivine, 25% mesostasis, and 1% high-μ phases. On a slice-by-slice basis, there are significant variations, especially in pyroxene, olivine, and mesostasis. Pyroxene abundances range from 36 to 75%, olivine from 0 to 36%, mesostasis from 15 to 38%, and high-μ phases from 0 to 3%. Such variation for modal abundances in nakhlites, and cumulate rocks in general, have been previously reported by [10–11].

CT fabric analysis: Overall, pyroxene and olivine display foliations (Fig. 1). The shape parameter T, which measures the type of fabric, also indicates a foliation in pyroxene and olivine (0.4 and 0.6, respectively). P', a measure of the degree of anisotropy, is 2.5 and 2.9 for pyroxene and olivine, respectively. All CT fabrics are also strongly aligned (<10°; Fig. 1).

3D CSD: The average long axis crystal length for pyroxene crystals measured in NWA 10645 is 1.58 mm, with a range of lengths from 0.45 to 3.68 mm. The 3D CSD slope is −1.49 or −1.06, and the *y*-intercept is 4.01 or 6.08 depending on the technique used, as determined by linear regressions (Fig. 2). There is a downturn at the smallest size bins and a negative slope regardless of the CSD technique used. Northwest Africa 10645 pyroxene residence times calculated using a growth rate of 10^{-10} $mm \cdot s^{-1}$ [12] is 213 or 299 Earth years, using a slope of −1.49 and −1.06, respectively.

Discussion: When conducting quantitative textural and petrofabric analyses for evaluating igneous processes, such as emplacement mechanisms and environments (e.g., intrusive versus extrusive), sample representativeness is imperative. Two dimensional modal abundances for NWA 10645 as determined by [2] overestimates the amount of pyroxene by 3% and underestimates olivine in the bulk sample by 13% when compared to our 3D modal abundances. Such discrepancy highlights the significance of using 3D techniques in petrologic studies.

Petrofabrics (e.g., foliations and lineations) can be used as indicators of emplacement styles. In igneous rocks, foliations may form during crystal accumulation or in the flattening regime of a lava flow [e.g., 13]. Moreover, a strong degree of alignment between CT fabrics has been suggested by [14] to be indicative of emplacement in shallow intrusive environments, like sills or dikes. Pyroxene and olivine in NWA 10645 both display foliation and a strong degree of alignment, suggesting NWA 10645 may be a candidate for emplacement in a shallow intrusive setting, consistent with the proposed emplacement settings for the nakhlites [e.g., 2].

Compared to traditional 2D CSDs, our 3D CSD slope is similar, but less than that for NWA 10645 (−1.61) as determined by [2] and the *y*-intercept (1.41) is nearly three to five log units higher. Variations in the CSD slopes and intercepts may be due to the difference in the crystals measured between 3D and 2D. By conducting a 3D CSD, we measure the true long axis of each pyroxene crystal, whereas with 2D CSDs, the true long axis of each crystal may not be measured due to the nature of how a thin section is cut. The 3D CSD slope also suggests a slower overall cooling rate, which is reflected in calculated residence times (2D = 184 Earth years [2]). However, the higher *y*-intercept in 3D may also be indicative of a higher nucleation density, which can occur with a considerable amount of undercooling [e.g., 15], consistent with minor element (e.g., Al and Ti) zonation in nakhlite pyroxene reported by [16].

Further work to conduct segmentations and quantitative textural and fabric analyses on all nakhlite and poikilitic shergottite X-ray CT scans are currently underway. By completing these analyses, we will ultimately provide better constraints on the formation and emplacement of martian meteorites.

References: [1] Udry et al. (2020) *JGR: Planets* 125, 1–34. [2] Udry and Day (2018) *GCA* 238, 292–315. [3] Rahib et al. (2019) *GCA* 266, 463–496. [4] Cnudde and Boone (2013) *Earth-Scie. Reviews* 123, 1–17. [5] Hanna and Ketcham (2017) *Chemie der Erde* 77, 547–572. [6] Ketcham and Ryan (2004) *J. of Microscopy* 213, 158–171. [7] Jelinek (1981) *Tectonophys.* 79, 63–67. [8] Eckley (2023) 86th MetSoc Meeting, ab.# 6271. [9] Ketcham (2005) *Geosphere* 1, 32–41. [10] Udry et al. (2012) *Met. Planet Sci.* 47, 1575–1589. [11] Corrigan et al. (2015) *Met. Planet Sci.* 50, 1497–1511. [12] Leu (2010) 42nd GSA Meeting. [13] Meurer and Boudreau (1998) *J. of Geology* 3, 293–304. [14] Eckley (2022) UT Austin Ph.D. Dissertation. [15] Higgins (2006) Quant. Text. in Ig. and Met. Petrology. [16] Ostwald et al. (2023) *LPSC LIV* ab.# 1123.